Low-Cost, Effective Vegetable Dehydration Powered by Solar Thermal and Photovoltaic Energy

João Garcia*, Arian Semedo**, João Pássaro***, Vitor Fernão Pires****‡

* Lisbon Superior Institute of Engineering, R. Conselheiro Emídio Navarro 1, 1959-007 Lisbon, Portugal

UnIRE, ISEL, Polytechnic University of Lisbon, Rua Conselheiro Emídio Navarro 1, Lisbon

MARE-IPS, Marine and Environmental Sciences Centre, Escola Superior de Tecnologia, Instituto Politécnico de Setúbal, Campus do IPS – Estefanilha, 2910-761, Setúbal, Portugal, Postal address

** UnIRE, ISEL, Polytechnic University of Lisbon, Rua Conselheiro Emídio Navarro 1, Lisbon

Department of Mechanical and Industrial Engineering (DEMI), Faculdade de Ciências e Tecnologias, Univer-sidade Nova de Lisboa, 2829-516 Caparica, Portugal,

*** ESTSetúbal-Instituto Politécnico Setúbal, Setúbal, Portugal

****‡ ESTSetúbal-Instituto Politécnico Setúbal, Setúbal, Portugal

INESC-ID, Lisboa

((joao.garcia@isel.pt, aa.semedo@campus.fct.unl.pt, jpap87@gmail.com, vitor.pires@estsetubal.ips.pt))

‡ Vítor Fernão Pires; vitor.pires@estsetubal.ips.pt

Received: 29.12.2024 Accepted:10.02.2025

Abstract- The preservation of food is essential in mitigating deterioration. Dehydration represents one of the most reliable techniques for extracting moisture from food. This method not only helps prevent spoilage and reduce post-harvest waste—an issue critical for small-scale farmers—but also proves to be economically advantageous by decreasing packaging and transportation costs. Additionally, it enhances food quality by retaining the majority of its nutrients. Several techniques, such as hot air drying, microwave-assisted drying, heat pump drying, and solar drying, are commonly utilized in the dehydration of vegetables. However, these methods are energy-demanding, prompting the need for more sustainable alternatives. Renewable energy solutions are necessary to minimize energy consumption while achieving comparable results. To address this challenge, a low-energy, portable, modular, and cost-effective dehydrator for fruits and vegetables was developed. This device primarily operates using solar energy but can also connect to the electrical grid when required, ensuring reliable functionality despite fluctuating environmental conditions. The development focused on optimizing the dehydration procedure by considering factors like product integrity, processing duration, costs, energy efficiency, and retention of flavor and aroma. The design was refined through iterative modelling using Computational Fluid Dynamics (CFD) simulations. This involved adjusting the air circulation velocity and temperature to accommodate the specific product being dehydrated, as well as real-time outdoor temperature and solar radiation conditions. The system's operation is further optimized by continuously monitoring the external humidity and temperature and adjusting its settings to fulfil the dehydration requirements. Another notable feature is the ability to function autonomously under ideal conditions, relying exclusively on solar energy, or with minimal electrical input when conditions are less favourable, thus significantly reducing overall energy demand.

Keywords Food preservation, energy-saving dehydration, solar energy utilization, sustainable drying techniques, reduction of post-harvest waste.

1. Introduction

Vegetable dehydration presents several challenges, including high energy consumption, dependence on fossil fuels, limited accessibility to efficient technologies, and significant post-harvest losses. In rural areas with restricted access to electricity from the public grid, traditional methods such as sun drying are frequently used, which can compromise product quality. On the other hand, electric alternatives are costly and have negative environmental impacts. Given these limitations, it is essential to develop low-cost and energy-efficient solutions, such as dehydration powered by solar thermal and photovoltaic energy, which contribute to reducing losses, improving product quality, and promoting sustainability, particularly in regions with limited access to electricity. This research aims to address these challenges by exploring innovative and sustainable methods for food dehydration. Food dehydration utilizing non-mechanical methods, such as the application of solar energy, is extensively used for products with a moisture content exceeding 2.5% [1,2], including items with moisture levels around 90%, such as fruits and vegetables. For example, watermelon has an approximate moisture content of 93% [3]. Food drying has served as a dependable and natural preservation technique since antiquity [3,4]. The adoption of renewable energy sources, especially solar power, for the dehydration and preservation of food has proven to be highly efficient [3,5], positioning it as one of the most beneficial methods, particularly in terms of energy conservation. Solar dehydration offers numerous advantages, including decreased processing time and energy expenditure [6], enhanced product quality [3,7], and a favourable environmental impact [8], as it avoids contributing to global warming by relying on renewable resources instead of fossil fuels [8,9]. The dehydration process removes water, allowing for extended food storage. This method is straightforward, cost-effective, and commercially viable, as it reduces the weight of packaging and transportation while extending the shelf life of the product [10]. Additionally, post-harvest losses are notably minimized, improving food quality and subsequently fostering economic growth and employment opportunities, provided that suitable drying technologies are applied [9,11]. The effectiveness of the dehydration process is influenced by three primary factors: temperature, relative humidity, and air velocity [12]. Temperature regulation is crucial for removing moisture from the food efficiently without damaging its thermal properties. The relative humidity of the air must be kept low to enhance the absorption of evaporated water [13,14]. Furthermore, the moisture-laden air must be continuously expelled from the drying chamber, which is achieved by controlling air velocity and ensuring uniform air distribution within the system. Food dehydration can be performed using solar radiation, electric dehydrators, or furnaces, with the appropriate operational parameters (temperature, humidity, and air velocity) applied based on the specific food being dehydrated [15,16]. Table 1 outlines the recommended temperature ranges for dehydration based on the type of horticultural product.

Table 1. Temperature ranges for dehydration of different horticultural products [adapted from 4]

Class of Horticultural Items	Drying Heat Temperature (°C)
Herbs	35
Vegetables	52
Fruits	57

The velocity of airflow during the dehydration process can reach up to 1.5 m/s [4,17]. Managing this factor is a significant advantage, as it directly impacts both the relative humidity of the air and the temperature within the drying chamber [15,17]. Several techniques exist to facilitate the dehydration of vegetables, including the application of heated air, microwave energy, ultrasonic waves, heat pump drying, and solar drying. A detailed review of these methods can be found in [18,19]. Nonetheless, in the current context, the adoption of renewable energy sources for this purpose is becoming an increasingly viable alternative, though there is limited research on this application. As heat generation is necessary for the process, the use of solar thermal and photovoltaic systems offers a promising solution. The adoption of renewable energy sources has been widely implemented across various applications, playing a crucial role in the transition towards a more sustainable energy system [20-22]. The integration of these technologies is essential for achieving the targets set by international energy and climate agreements, fostering the reduction of carbon emissions and decreasing reliance on fossil fuels [23-24]. The combined use of solar thermal and photovoltaic systems has been extensively studied and applied in various fields, including air-source heat pumps, refrigeration systems, and combined heat and power systems [25-27]. This study will concentrate on vegetable dehydration, specifically focusing on a system powered by renewable energy. The aim is to design a low-energy dehydrator for fruits and vegetables that is portable, modular, and cost-effective. To eliminate reliance on non-renewable energy sources, a system was developed that operates solely on solar thermal and photovoltaic energy.

2. Dehydration Through Solar Energy

2.1. Fundamental Principles

Solar dehydration employs solar radiation to increase air temperature, enabling the removal of moisture from food products. During this process, the dehydrated materials undergo modifications in both their structural properties and nutritional composition due to heat and mass transfer phenomena [5,17]. To achieve high efficiency, advanced solar collection systems, such as solar collectors, are required. As the air is heated, its relative humidity decreases, allowing it to absorb and transport the moisture released by the food. The controlled movement of air within the drying chamber is essential to facilitate moisture removal and enhance the drying process. The dehydration mechanism consists of two distinct phases. The initial phase involves the evaporation of surface moisture from the food’s outer layers. In the subsequent phase, internal moisture migrates from the deeper layers toward the surface, where it evaporates. Figure 1 presents a schematic representation of these two dehydration stages.

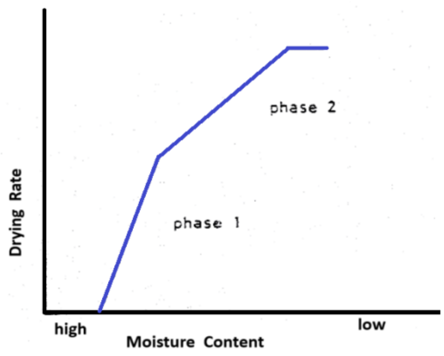

Fig. 1. Drying rate versus moisture content [adapted from 5].

2.2. Categorization of Solar Dehydrators

Solar dehydrators are categorized into two main types based on the presence or absence of mechanical airflow assistance. Systems that do not incorporate mechanical components for air circulation are classified as passive dehydrators, whereas those that utilize mechanical devices, such as fans or pumps, are referred to as active dehydrators. Passive dehydrators are further divided into direct and indirect types [7]. The key distinction between these two systems lies in whether the food is directly exposed to solar radiation (direct passive dehydrators) or shielded from it (indirect passive dehydrators). Figure 2 illustrates the different classifications of solar dehydrators [5].

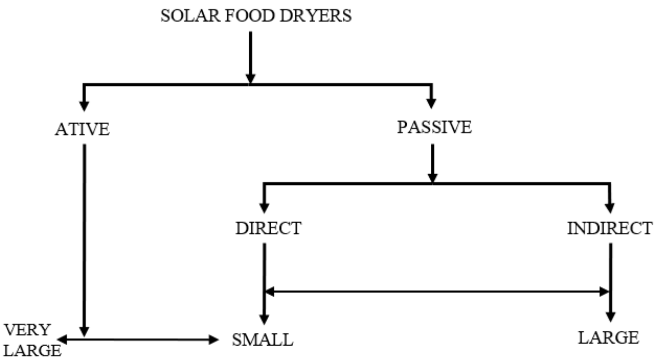

Fig. 2. Categorization of Solar Dehydration Systems [adapted from 5].

In direct solar dehydrators, the drying chamber is enclosed with transparent materials such as glass or plastic, incorporating vents to facilitate air circulation. Conversely, in indirect passive solar dehydrators, the food is placed inside a well-insulated drying compartment, where a solar collector is used to heat incoming air, reducing its relative humidity and enhancing moisture absorption. In these systems, air circulation occurs through natural convection, with external air intake positioned at a lower level than the exhaust outlet to promote airflow efficiency. For active solar dehydrators, air movement is mechanically controlled using a small fan or, in larger-scale systems, an air circulation pump to distribute heated air uniformly. From a thermodynamic perspective, active systems demonstrate higher efficiency by accelerating the dehydration process [6], enabling the simultaneous drying of larger quantities of food. Studies indicate that active dehydrators can reduce drying time by up to 1.5 times compared to passive systems while maintaining environmental sustainability, as they do not produce harmful emissions [6].

2.3. Potential Challenges of Solar Dehydrators

Although solar dehydration is a widely used and cost-effective technique in the food industry due to its simplicity compared to other drying methods [7], it presents certain limitations, primarily related to the requirement for elevated temperatures. Excessive heat exposure often results in a decrease in the water absorption capacity and bulk density of fruits and vegetables, leading to nutrient degradation, alterations in flavor and texture, and undesirable physical and biochemical changes [4,6,7]. Additionally, direct solar dehydration can be an inefficient and inconsistent process, as it heavily depends on meteorological conditions. The absence of solar radiation during nighttime further limits its operational continuity, increasing the total drying time and potentially compromising product quality. Given these constraints, integrating solar energy with a complementary energy source emerges as an optimal solution to enhance process reliability and ensure consistent dehydration performance, regardless of weather variations.

3. The Innovative Solar Dehydrator

3.1. Overview of the Proposed System

The proposed solar dehydrator was developed with the aim of ensuring continuous operation regardless of climatic conditions, through the utilization of renewable energy sources, namely thermal and photovoltaic solar power. By harnessing solar energy, this equipment offers an efficient and sustainable solution for the dehydration of fruits and vegetables, adapting to varying weather conditions while contributing to the reduction of non-renewable energy consumption. Furthermore, when available solar energy is insufficient for continuous operation, the dehydrator can switch to conventional electrical power, ensuring its operation even during prolonged periods of low solar irradiance. The dehydration system is composed of a drying chamber connected to a solar thermal collector, a photovoltaic panel, an electric heating element, fans for improved air circulation, motorized actuators or valves for regulating air dampers, as well as temperature and humidity sensors. An automation system is also included to maintain optimal operational conditions. The thermal solar energy, captured by the solar panel, is used to heat the air circulating inside the dehydration chamber, contributing to the drying process of the products, provided that climatic conditions allow. The photovoltaic (PV) panel, in turn, supplies electrical power to charge the batteries that power the auxiliary devices of the dehydrator, such as air circulation fans, the system controller, heating elements, and motorized actuators. This utilization of solar energy to charge the batteries is essential for ensuring the self-sustaining operation of the equipment during the day, maximizing the use of renewable energy and minimizing dependence on the electrical grid. When solar energy is insufficient to maintain the desired temperature in the chamber, the system relies on the electric heating element, which works in conjunction with the solar panel to ensure that the air is heated to an optimal level for dehydration. This heating element operates only when necessary, contributing to efficient energy management. The use of solar heating as the primary energy source enhances the sustainability of the system, with the electric resistance serving as a supplementary solution, activated only when climatic conditions are unfavourable. Additionally, the system is designed to optimize air circulation within the dehydration chamber. The fans, controlled by the system, allow for the adjustment of air flow speed, promoting uniform and efficient dehydration. The register actuator is responsible for regulating the intake and exhaust of air, controlling the internal conditions of the chamber. Temperature and humidity sensors constantly monitor the environmental parameters, ensuring that the dehydration process remains efficient and within the required levels. The control module centralizes all system functions, monitoring and adjusting temperature, humidity, air speed, and airflow, ensuring that all components operate in a coordinated and efficient manner. This intelligent control system contributes to the sustainability of the dehydrator by optimizing resource usage, minimizing energy waste, and ensuring the efficiency of the dehydration process. In summary, the proposed solar dehydrator is an efficient and sustainable solution that predominantly utilizes renewable energy and resorts to conventional energy only when necessary, ensuring continuous operation while reducing the environmental impact associated with the dehydration of fruits and vegetables. A schematic of the proposed system is presented in Figure 3.

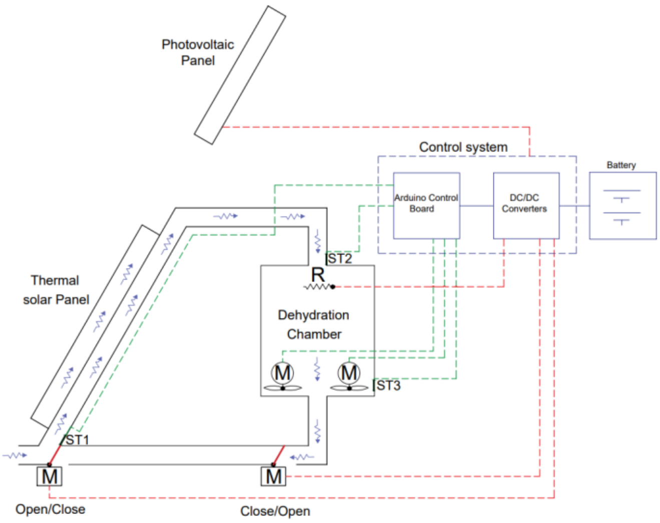

Fig. 3. Scheme of proposed system.

The system is governed by DC-DC converters and an Arduino control board. These converters manage the energy provided by the photovoltaic panel and control the operation of the DC motor fans and heating resistor. The control mechanism incorporates several temperature and humidity sensors located both inside and outside the system, along with motorized actuators/valves and fans to regulate the optimal conditions within the dehydration chamber for efficient food drying. The Arduino control board, equipped with a microprocessor, oversees the coordination of these components.The system uses DHT22 model sensors for temperature and humidity, and a set of four 12 V fans connected in parallel, which are controlled via a 24 V Pulse Width Modulation (PWM) signal, supporting a 50W heating resistor.The motorized actuators/valves operate at 24 V and are controlled by position feedback from a 0-10 V analog input, with this control voltage being generated through PWM outputs functioning as a digital-to-analog converter (DAC). The hardware control functions were programmed using the open-source Arduino IDE 1.6.11 software. The critical parameters monitored in this system include Temperature (T, °C), Relative Humidity (RH, %), and Air Velocity (V, m/s). The dehydrator described in this work can adjust these three parameters, with two being actively controlled (temperature and air velocity) and one passively controlled (relative humidity). This design helps prevent product degradation due to environmental factors such as wind, rain, dust, moisture, and animal interference, unlike open-air sun drying (OASD) and direct sunlight drying (DSD). Furthermore, the risk of biochemical or microbiological contamination is significantly minimized [10].

3.2. Optimization of the Process

Optimizing the dehydration process requires balancing several factors, including product quality, drying time, operational cost, energy efficiency, and preservation of flavor and aroma. The developed dehydration system is capable of enhancing all these aspects by regulating the air temperature and airflow velocity during the drying process, which are adjusted based on external conditions such as ambient temperature, solar radiation, and the specific type of food being dehydrated. Optimization is achieved by monitoring both the external environmental parameters (temperature and humidity) and the internal conditions (inlet and outlet air within the dehydration chamber). The control system uses this information to manage the balance between recirculated air and fresh airflow, ensuring the most efficient and effective drying conditions.

3.3. Eco-Friendly Design and Assembly

The equipment was designed and assembled with sustainability in mind, utilizing environmentally conscious materials and avoiding the use of adhesives, coatings, or any hazardous surface treatments. All joining and fastening methods are purely mechanical, further promoting an eco-friendly and safe construction.

3.4. Mobility of the Equipment

The equipment is lightweight and equipped with fully adjustable wheels, making it easy to position and orient. This flexibility in movement enables the system to be placed optimally for maximum solar efficiency, taking advantage of the ideal solar orientation based on solar time, and adjusting to the specific needs of the production process at any given time.

3.5. Principle of Operation

The effectiveness of the dehydration process is contingent upon the precise regulation of several variables within the chamber: relative humidity, air temperature, airflow velocity, and the adjustment of air register positions. These parameters are controlled by the system's central controller. The process involves circulating heated air around the food arranged on the shelves within the dehydration chamber. Ideal operating conditions are generally characterized by high temperatures, moderate airflow, and low relative humidity. Inside the chamber, it is critical to ensure the continuous circulation of warm air with low moisture content.A key innovation of this system is its ability to alternate between using external fresh air or recirculated air within the chamber, depending on the weather conditions. The system can function with solely fresh air, a mix of fresh and recirculated air, or completely recirculated air, with the specific air type selected based on the position of the actuators and motorized valves (as depicted in Figure 4).Further enhancing the system's flexibility, it is equipped with variable-speed fans. These fans can be adjusted to facilitate either rapid dehydration, which shortens the drying time, or slower dehydration, which may improve the flavor and aroma of the food. The fans are essential for controlling the airflow velocity to achieve the desired dehydration results.Regarding energy usage, the dehydrator operates in a hybrid mode, primarily utilizing renewable energy when conditions are favorable. In cases of adverse weather, the system switches to conventional electrical power, ensuring the dehydration process remains consistent and efficient, while minimizing overall energy consumption.

External Air Configuration

The system enters the 100% external air (fresh air) mode (Figure 4-a) when favorable environmental conditions are met, including high temperatures, gentle winds, and low humidity, typically observed during dry or summer periods. In this setting, the outside air is drawn in through an intake at the bottom of the solar panel. Due to solar radiation, the air rises naturally via convection and reaches the entry point of the dehydration chamber. Within the chamber, the air is circulated primarily through natural convection, supplemented by air blowers situated at the lower part of the chamber, which direct the air outward.The intake vents at the base of the solar panel are activated to allow fresh air to enter, while the exhaust vents downstream of the air circulation fans are also triggered to expel the air. These vents are controlled by two motorized actuators/valves, which are managed by the system's controller.

Air Recirculation Mode

When external conditions are not suitable for using 100% fresh air, such as in winter or during cold, overcast, and relatively dry weather, the system switches to recirculating air within both the chamber and the solar panel (Figure 4-b). In this scenario, the air flows through the system, rising within the solar panel due to natural convection induced by solar radiation, reaching the inlet of the dehydration chamber. Inside the chamber, the air is pushed downward by fans located at the lower section, and it is then cycled back to the intake of the solar panel.During this process, the intake and exhaust vents are sealed, preventing external air from entering and internal air from exiting, until the sensors detect that the circulating air has become saturated with moisture. At this point, the air must be replaced with drier air from the outside, even if it is cooler. If the desired temperature inside the chamber cannot be achieved by the thermal solar panel alone, it can be supplemented by the heating element.

Combined Air Mode

The hybrid air mode is intended for conditions that are neither excessively cloudy nor humid. In such cases, a portion of the recirculated air is reused, while fresh air is introduced into the dehydration chamber, creating a mixture of both air sources. This combination of recirculated and fresh air rises through the solar collector, propelled by natural convection induced by solar radiation heating the collector (and potentially the heating element), and subsequently reaches the intake of the dehydration chamber. The fans positioned at the lower part of the chamber guide the air downward.To allow for the replacement of some of the air with fresh air, the intake vent at the bottom of the chamber is engaged, while the remaining air is directed toward the solar panel intake, where it mixes again with fresh air. The control unit regulates the dampers according to the readings from the temperature and humidity sensors, ensuring proper management of the inlet and outlet airflow (see Figure 4-c).

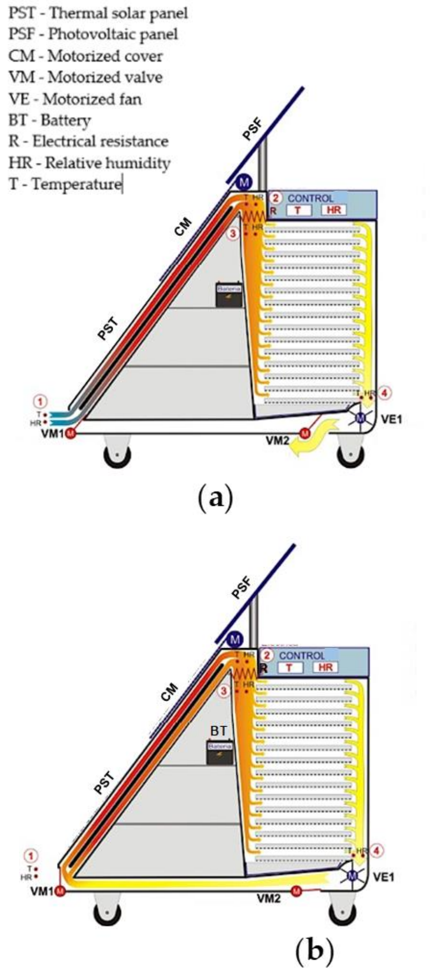

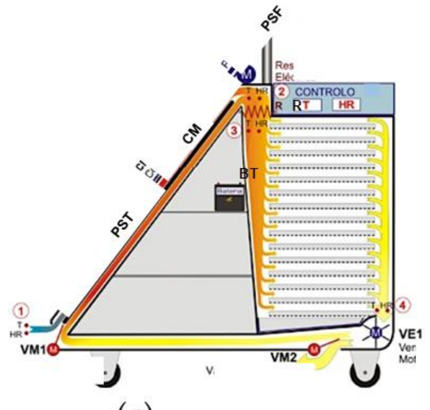

Fig. 4. Functioning modes: (a) external air setting; (b) recirculated air setting; (c) mixed air setting.

4. Simulation of Fluid Dynamics Using Computational Methods

4.1. Overview

The design of the dehydration chamber was subjected to a computational fluid dynamics (CFD) simulation to explore and optimize the efficiency of the dehydration process. ANSYS Fluent software [6] was selected to carry out this detailed numerical analysis, focusing on examining and refining the airflow patterns and distribution within the drying compartment to enhance overall drying performance.

4.2. Simulation Model

Two models based on turbulence equations can be used to calculate the characteristic scales of turbulence by solving two independent transport equations. Since Launder and Spalding proposed it, the conventional k-model in ANSYS Fluent has been the go-to tool for real-world engineering flow calculations. [28]. The widespread adoption of this model in industrial simulations of flow and heat transfer is due to its robustness, cost-effectiveness, and sufficient accuracy across a wide variety of turbulent flows. Recognized as a semi-empirical method, the model's equations are based on phenomenological principles and empirical data. he standard model utilizes transport equations for turbulent kinetic energy (k) and its dissipation rate (ε) [29-31]. The exact equation is used to form the model's governing equation, while the governing equation itself was created through physical reasoning, without direct reference to its mathematically accurate equivalent. As the model assumes fully turbulent flow with minimal influence from dynamic molecular viscosity, it is only applicable to entirely turbulent flows. To overcome this limitation, the RNG model was introduced to improve the simulation model's performance [32-34].

4.3. Boundary conditions Specifications

To develop a prototype, the numerical simulation concentrated primarily on the dehydration chamber, specifically the airflow within it. Temperature serves as the central driving factor in the dehydration process, with the even distribution of heat throughout the chamber being essential. This uniformity is facilitated by the airflow, which is a crucial element for ensuring effective food processing. It guarantees consistent dehydration, preserving the properties and quality of all products placed on various shelves. With this goal in mind, the following initial boundary conditions were established: Inlet flow velocity: 0.1 and 2.9 m/s for different scenarios; and Outlet conditions: Outflow.

4.4. Simulation Outcomes

The computational fluid dynamics (CFD) simulation enabled the analysis of airflow velocity distribution within the dehydration chamber, allowing for the verification of the correct placement of equipment to maximize system efficiency. Figure 5 presents the numerical simulation results, highlighting variations in air velocity and its distribution throughout the chamber.

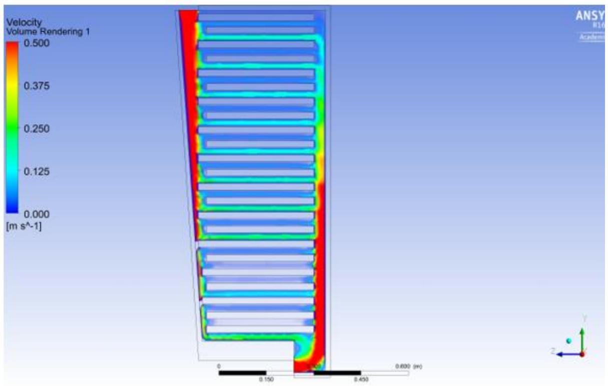

Fig. 5. CFD velocity results.

The results indicated that the airflow velocity inside the chamber remained below 1.5 m/s, with even lower values near the shelves containing the product, where velocities below 0.375 m/s were recorded. As expected, an increase in velocity was observed in the area near the fan, reaching approximately 0.5 m/s at both the chamber inlet and outlet. This velocity distribution suggests a relatively uniform airflow, promoting an efficient drying process without excessive particle displacement or significant variations in moisture removal rates.The analysis of different scenarios allowed for the optimization of the dehydration chamber configuration, including the arrangement of shelves and airflow direction. The controlled distribution of air velocity proved essential in ensuring an adequate drying gradient, preventing stagnation zones, and guaranteeing uniform food dehydration. These findings highlight the importance of CFD simulation in assessing and improving the thermal and aerodynamic performance of the system, contributing to a more efficient and homogeneous dehydration process.

5. Preliminary Prototype

The refinements in the dehydration chamber, derived from the optimization process via the CFD model, enabled the creation of an upgraded preliminary prototype, now ready for evaluation. Figure 6 illustrates (a) an image of the physical prototype and (b) its associated design blueprint.

Table 2 presents a detailed list of the components used in the development of the solar-powered system. These components include structural elements, solar panels, electrical components, and the movement system, with each playing a specific role within the overall system design.

Table 2. List of components used in the solar dehydrator system

Item	Description	QTY
Structure	Bracket , Tube Various and Cardboard dimensions (Aluminum)	39
PV Panel	"Solar World" Sw100poly RGP, 100W, 24VDC	1
Voltage Regulator	"LCD PWM" CM1024, 12-24V, 10A	1
Thermal Solar Panel	Manual fabrication (Corner, Aluminum Sheet, Aluminum Mesh, Transparent Acrylic Plate)	1
Resistance	50W, 24VDC	1
Batteries	"Ultracell" UCG20-12, 12V, 20Ah	2
Sensor	DHT22	4
Resistance Controller	12V relay	1
Arduino	Arduino R3	1
Fan Control	Titan TFD-6020M12B, 12VDC	4
Valve Controller and Pow. Supp.	74164; 7805; 7905	2
Support Wheels	Rotating wheels with brake and without brake	4
Aluminum Mesh	For trays	2
Titan Fan	12VDC	4

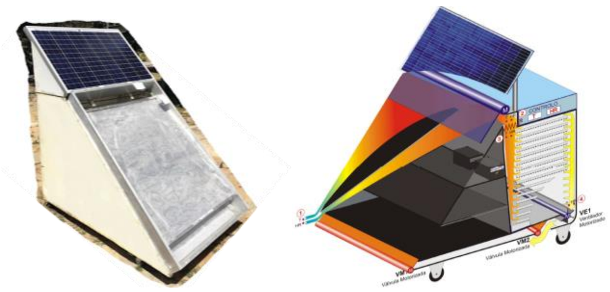

(a) (b)

Fig. 6. Combined solar dehydration system for horticultural products: (a) photograph; (b) diagram.

5.1. Operational Test

The present study aimed to evaluate the performance of the solar dehydrator under real operating conditions. The test was conducted on September 6, 2023, starting at 11:00 AM and concluding at 5:30 PM. The equipment was placed outdoors at 10:30 AM to ensure direct exposure to solar radiation. The setpoint temperature was established at 50°C, with the electrical resistance activated after 10 minutes, requiring approximately 20 minutes to reach the desired temperature. The test was carried out using two shelves containing food for dehydration, one positioned at the intermediate level and the other at the upper position within the drying chamber.The recorded values throughout the test period are presented in Table 3, including the temperatures measured at different points in the system (T1, T2, T3, and T4), the relative humidity of the air (H3 and H4), the status of the electrical resistance, the type of air intake, and the speed of the air flow regulators.

Table 3. Temperature, humidity, and system parameters recorded during the operational test

Measurement	Time	T1 (°C)	T2 (°C)	T3 (°C)	T4 (°C)	H3 (%)	H4 (%)	Resistance	Air Intake	Airflow Regulator Speed (%)
1	11:00	31.3	60.3	49.4	35.7	-	-	On	Recirculation	0
2	11:15	31.4	61.6	50.8	36.0	-	-	Off	Recirculation	4
3	11:25	32.6	61.3	52.0	36.8	-	-	Off	Recirculation	9
4	11:35	35.6	60.4	52.5	39.9	-	-	Off	External	19
5	11:45	33.1	59.5	52.7	40.1	-	-	Off	External	24
6	11:55	35.6	63.2	54.8	42.7	-	-	Off	External	39
7	12:05	33.4	64.1	55.3	43.3	-	-	Off	External	43
8	12:15	30.9	62.6	52.8	43.4	-	-	Off	External	58
9	12:30	33.5	62.3	50.8	42.1	-	-	Off	External	68
10	12:45	34.4	62.6	48.0	38.2	-	-	Off	External	82

Table 3. (continued)

11	13:00	31.4	62.8	49.5	36.8	-	-	Off	External	78
12	13:30	32.6	62.2	50.1	37.7	12.3	33.5	Off	External	100
13	14:00	32.2	64.6	51.6	37.9	10.1	30.0	Off	External	100
14	14:30	34.6	62.4	52.7	38.6	9.1	28.7	Off	External	100
15	15:00	37.6	62.9	52.7	39.9	9.5	25.7	Off	External	100
16	16:00	39.6	63.7	52.7	41.8	8.9	22.6	Off	External	100
17	16:40	41.7	64.2	54.8	43.6	7.0	19.5	Off	External	100
18	17:00	41.7	65.0	56.0	43.5	5.0	16.9	Off	External	100
19	17:15	38.4	63.7	55.3	43.0	5.4	17.1	Off	External	100
20	17:30	37.2	62.0	54.7	42.2	5.4	17.9	Off	External	100

The results of the operational test of the solar food dehydrator indicate good system performance. Measurements of temperature (T1 to T4) and relative humidity (H3 and H4) showed that the solar thermal panel was effective in heating the air, with the panel's output temperature (T2) ranging from 60.3°C to 65.0°C throughout the day, while the inlet temperature to the drying chamber (T3) ranged from 48.0°C to 56.0°C, values suitable for the dehydration process. The relative humidity at the inlet of the chamber (H3) was maintained between 5.0% and 12.3%, creating an environment conducive to the removal of water from the food, while the relative humidity at the chamber outlet (H4) ranged from 5.4% to 17.9%. The difference between these relative humidity values demonstrates the effectiveness of the dehydration process, as the removal of water from the food directly leads to a reduction in the humidity at the chamber's exit. The electrical resistance was deactivated, indicating that the solar system was sufficient to heat the air without the need for external energy sources, and the fan speed was adjusted as necessary, reaching 100% in the later measurements, which facilitated moisture removal. These results demonstrate that the solar dehydrator is efficient, autonomous, and viable as a sustainable solution for food drying, depending on the available solar radiation.

Table 4. Pre- and post-dehydration moisture content results (Eggplants)

Moisture content (%)	Test 1	Test 2	Test 3	Test 4	Test 5
Fresh	92,3	91,8	93,1	91,9	92,1
Dried	2,1	1,9	2,2	1,7	1,7

The results presented in the table demonstrate the effectiveness of the dehydration process applied to eggplants. It is observed that the initial moisture content of the fresh products varied between 91.8% and 93.1%, typical values for this type of food. After the dehydration process, the final moisture content was reduced to a range between 1.7% and 2.2%, indicating a significant removal of water. These values suggest that the dehydrator could achieve moisture levels suitable for food preservation, as a moisture content below 5% is generally recommended to prevent microbial growth and ensure the stability of the stored product. Furthermore, the low variation in results across different tests suggests consistent performance of the system, demonstrating its efficiency and repeatability in the drying process. The significant reduction in moisture confirms the feasibility of the equipment for eggplant processing, making it an efficient solution for extending the product's shelf life without compromising quality. Figure 7 shows the result of the final product.

Fig. 7. Final view of eggplants dehydrated.

5.2. Efficiency of the Tested Dehydrator

The efficiency of the dehydrator was calculated based on the reduction in relative humidity of the eggplants during the dehydration process. The formula used to calculate the dehydration efficiency is as follows:

$$\eta_d = \left(\frac{RH_i - RH_f}{RH_i}\right) \cdot 100\% \quad (1)$$

Where: RH_i is the relative humidity of the product before the dehydration process.

RH_f is the relative humidity of the product after the dehydration process.

The table 5 shows the dehydration efficiency for each of the five tests conducted.

Table 5. Dehydration efficiency (%) for each test and the average

Test	1	2	3	4	5	Average
Efficiency (%)	97.7	97.9	97.6	98.1	98.2	97.9

From the results, it is evident that the dehydrator performs highly effectively, with an average dehydration efficiency of 97.9% across all five tests. This high efficiency demonstrates the system's ability to remove moisture effectively from the eggplants, which is essential for preserving food quality and preventing microbial growth during storage. These results also indicate that the dehydrator operates consistently, with only slight variations in efficiency between the tests (ranging from 98.2% to 97.6%). Such consistency is crucial for ensuring the reliability and quality of the dehydration process.

5.3. Efficiency of the Solar Panel

The thermal efficiency of a solar thermal panel is a key performance indicator that determines how effectively the panel converts incident solar energy into usable thermal energy. To calculate the efficiency, we need to account for the energy absorbed from the sun and the amount of that energy which is effectively transferred to the air passing through the panel.

$$\eta_{solar\ panel} = \left(\frac{Q_{useful}}{Q_{in}}\right) \cdot 100\% \quad (2)$$

Where: Q_{useful} is the useful thermal energy provided to the air.

Q_{in} is the incident solar energy that is absorbed by the panel.

The useful thermal energy, Q_{useful}, is calculated using the following formula:

$$Q_{useful} = m \cdot cp \cdot \Delta T \quad (3)$$

Where: *m* is the mass flow rate of air (kg/s), which can be determined from the volumetric flow rate and the air density.

Cp is the specific heat capacity of air (approximately 1014 J/(kg·°C)).

ΔT is the temperature difference between the air leaving the panel (T2) and the air entering the panel (T1).

The incident solar energy absorbed by the panel, Q_{in} is calculated as:

$$Q_{in} = G \cdot A \cdot t \quad (4)$$

Where: *G* is the solar irradiance (W/m^2), which is the power received per unit area.

A is the area of the solar thermal panel (m^2).

t is the period during which the solar energy is received (in seconds).

Table 6 presents the values obtained for the calculation of useful thermal energy, while Table 7 provides the values used to determine the incident solar energy.

Table 6. Useful thermal energy

Q_{useful}	*m* (kg/s),	*Cp* kJ/(kg°C)	ΔT
20.8408	0.7340	1.014	28

Table 7. Incident solar energy

Q_{in} (kW)	G (KW/m^2)	A (m^2)	t (s)
35.7246	1.115	1.602	20

The average thermal efficiency of the solar panel was 58.36%, falling within the expected range for glazed flat-plate collectors (50% to 70%). This performance demonstrates an efficient conversion of incident solar energy into useful heat, making it comparable to conventional systems. In contrast, vacuum tube collectors can achieve higher efficiencies (60% to 80%), albeit at a higher cost.

5.4. Energy Generation by the Photovoltaic Panel

The photovoltaic (PV) system employed in this study consists of a “Solar World” SW100poly RGP solar panel with a rated power of 100 W and an output voltage of 24 VDC. The system also includes a charge controller (“LCD PWM” – CM1024, 12-24V, 10A) and a battery storage unit composed of two Ultracell UCG20-12 gel batteries (12V, 20Ah each). The energy generated by the PV panel is used to power various components of the dehydrator, including the actuator, ventilation system, heating element, and control module. The energy output of the PV panel can be estimated using the following equation:

$$E_{PV} = P_{PV} \cdot t \quad (5)$$

Where: E_{pv} is the total energy generated (Wh).

P_{pv} is the rated power of the panel (100 W).

t is the effective duration of solar exposure (hours).

Taking into account an average of 5 peak sun hours per day, the total daily energy generated by the photovoltaic panel is:

$$E_{PV} = 100\text{W} \cdot 5\text{h} = 500\text{Wh}$$

This energy is then stored in the battery system or directly consumed by the dehydrator's electrical components. The main electrical consumers in the system include the actuator (Eletro Controls Limited – E16-24M, 24VAC/VDC) with a power consumption of 5.2 W, the ventilation system (Titan TFD-6020M12B, 12VDC) consuming 2.04 W, the resistance (50W, 24VDC) with a 50 W power demand, and the control module (Arduino, 24VDC) requiring 2.5 W. Assuming continuous operation for 5 hours per day, the total daily energy consumption of these components is calculated as follows:

$$(5.2 + 2.04 + 50 + 2.5) \cdot 5\text{h} = 298.7\ \text{Wh/day}$$

Thus, the total daily energy consumption of these components is approximately 298.7 Wh/day. The system utilizes two Ultracell UCG20-12 gel batteries (12V, 20Ah each). The total energy storage capacity of the battery bank is given by:

$$E_{battery} = 2 \cdot 12\text{V} \cdot 20\text{Ah} = 480\text{Wh}$$

The total daily energy consumption is 298.7 Wh/day, and the total battery capacity is 480 Wh. The number of days the system can operate on battery power, without recharging, is:

$$\text{Operating days} = \frac{\text{Baterry capacity}}{\text{Energy consumpton per day}} \quad (6)$$

$$\text{Operating days} = \frac{480\text{Wh}}{298.7\ \text{Wh/day}} = 1{,}61\ \text{days}$$

With the two Ultracell UCG20-12 gel batteries, the system can sustain operation for approximately 1.61 days without needing recharging, ensuring the system can continue functioning even during periods of low solar irradiation.

6. Conclusion

This article presents a novel vegetable dehydration system based on renewable sources, designed to be energy-efficient, cost-effective, mobile, and modular. The system utilizes solar energy, both thermal and photovoltaic, operating in a hybrid manner, which allows it to function independently of weather conditions. The prototype was optimized in terms of process duration, product integrity, energy performance, and sensory characteristics, adjusting the drying air temperature and circulation velocity according to environmental conditions and the nature of the product. This approach significantly contributes to sustainability by promoting the use of clean energy sources, reducing reliance on fossil fuels, and lowering the carbon footprint associated with the dehydration process.The system's efficiency was demonstrated by experimental results, which indicated a reduction in the moisture content of eggplants from 91.8–93.1% to 1.7–2.2%, values suitable for food preservation. The average dehydration efficiency was 97.9%, with minimal variations across tests, demonstrating the system's consistency and reliability. The thermal efficiency of the solar panel was 58.36%, falling within the expected range for glazed flat-plate collectors.Additionally, the photovoltaic system, through the integrated battery, allows the system to operate for 1 day and 14 hours without recharging, ensuring autonomy and continuity even during periods of low solar irradiation. These results confirm the system's viability as an efficient and sustainable solution for eggplant dehydration, contributing to the reduction of food waste and extending the product's shelf life while maintaining its quality. The system aligns with more responsible production practices and promotes environmental preservation.

Acknowledgements: Gratitude is expressed for the valuable administrative and technical contributions provided by all the unmentioned contributors during the development of this work.

References

[1] D. S. Jayas, "Food Dehydration", Food Science, https://doi.org/10.1016/B978-0-08-100596-5.02913-9, ISBN9780081005965, Elsevier, 2016.

[2] M. Das, E. K. Akpinar, "Investigation of Pear Drying Performance by Different Methods and Regression of Convective Heat Transfer Coefficient with Support Vector Machine". Applied Sciences, vol. 8, no. 2, p. 215, 2018. https://doi.org/10.3390/app8020215

[3] P. Udomkun, S. Romuli, S. Schock, B. Mahayothee, M. Sartas, T. Wossen, E. Njukwe, B. Vanlauwe, J. Müller, "Review of solar dryers for agricultural products in Asia and Africa: An innovation landscape approach", Journal of Environmental Management, vol. 268, p. 110730, August 2020, 110730.

[4] Y. Baraday, M. Howlader, A. Ismail, M. Hrairi, "Chapter 6 - Drying of Fruits and Vegetables: The Impact of Different Drying Methods on Product Quality. In Advances in Heat Pump-Assisted Drying Technology", Editor Vasile Minea, CRC Press, 2015.

[5] A. Patel, A. Shah, H. Bhargav, "Review on Solar Dryer for Grains", Vegetables and Fruits", International Journal of Engineering Research & Technology, vol. 2, no. 1, pp. 1-7, January 2013.

[6] R. Boyer, K. Huff, "Using Dehydration to Preserve Fruits", Vegetables, and Meats. Virginia Tech, pp. 348–597, 2008.

[7] R. Gregoire, "Understanding Solar Food Dryers", Volunteers in Technical Assistance (VITA): Virginia, United States of America, 2009.

[8] P. Kendall, P. Dipersio, J. Sogos, "Drying Vegetables. In Preserving Food: Drying Fruit and Vegetables". University of Georgia Cooperative Extension Service. College of Family and Consumer Science in cooperation

with the College of Agricultural and Environmental Science, 2012.

[9] Y. Baradey, M.N.A. Hawlader, A.F. Ismail, M. Hrairi, "Chapter 6, Drying of Fruits, and Vegetables: The Impact of Different Drying Methods on Product Quality", Book Advances in Heat Pump-Assisted Drying Technology, 2015.

[10] R. Karabacak, Ö. Atalay, "Comparison of drying characteristics of tomatoes with heat pump dehumidifier system", solar-assisted system, and natural drying. Journal of Food, Agriculture & Environment, vol. 8, no. 2, pp. 190 – 194, 2010.

[11] R. Daghigh, K. Spoian, M. H. Ruslan, A. Alghoul, C.H. Lim, S. Mat, B. Ali, M. Yahya, A. Zahraim, M.Y. Sulaiman. "Survey of Hybrid Solar Heat Pump Drying Systems". Proceedings of the 4th IASME/WSEAS International Conference on Energy & Environment (EE'09), 2009.

[12] S. K. Chin, C. L. Law, "Optimization of Convective Hot Air Drying of Ganodermalucidum Slices Using Response Surface Methodology". International Journal of Scientific and Research Publications, vol. 2, no. 5, 2012.

[13] H. Qing-guo, Z. Min, A. S. Mujumdar, D. Wei-hua, S. Jin-cai. "Effects of Different Drying Methods on the Quality Changes of Granular Edamame", Drying Technology, vol. 24, pp. 1025–1032, 2006.

[14] H. Vega-Mercodo, M. Gongora-Nerto, G.N. Barbora-canovas. "Advances in dehydration of food", Journal of Food Engineering. vol. 49, pp. 271-289, 2001.

[15] C. Tortoe, "A review of osmo dehydration of food industry", African Journal of Food Science, vol. 4, no. 6, pp. 303 – 324, 2010.

[16] M. Hawlader, C. O. Perera, M. Tian. "Heat Pump Drying Under Inert Atmosphere", Proceedings of the 14th International Drying Symposium (IDS2004), vol. A, pp. 309-316, August 2004.

[17] S. Jangam, C. L. Law, A. S. Mujumdar, "Drying Foods, Vegetables and Fruits". ISBN978-981-08-7985-3, 2010.

[18] V. Sagar, P. Kumar, "Recent advances in drying and dehydration of fruits and vegetables: a review", Journal of Food Science and Technology, vol. 47, pp. 15–26, February 2010.

[19] M. Nowacka, M. Dadan, U. Tylewicz, "Current Applications of Ultrasound in Fruit and Vegetables Osmotic Dehydration Processes", Applied Sciences, vol. 11, no. 3, p. 1269, January 2021, https://doi.org/10.3390/app1103126.

[20] S. Belgana, A. Dabib, H. Bilil, M. Maaroun, "Hybrid renewable energy system design using multobjective optimization," in 2013 International Conference on Renewable Energy Research and Applications (ICRERA), pp. 955–960, October 2013, doi: 10.1109/ICRERA.2013.6749890.

[21] L. S. Paragond, C. P. Kurian, B. K. Singh, "Design and simulation of solar and wind energy conversion system in isolated mode of operation," in 2015 International Conference on Renewable Energy Research and Applications (ICRERA), pp. 999–1004, November 2015, doi: 10.1109/ICRERA.2015.7418560.

[22] B. Dollinger, K. Dietrich, "Storage systems for integrating wind and solar energy in Spain," in 2013 International Conference on Renewable Energy Research and Applications (ICRERA), pp. 361–365, October 2013, doi: 10.1109/ICRERA.2013.6749781.

[23] K. Sarah, K. Eokedu, R. Uhunmwangho, "Harnessing Solar and Wind Power for Hybrid Stand-alone Energy System: The Case of Coastline Communities in Delta State of Southern Nigeria," International Journal of Smart Grid, vol. 7, no. 1, pp. 1-13, March 2023.

[24] B. Adebanji, A. Osalade, S. Adeleye, T. Fasina, A. Abe, C. Okafor, "Economic and Environmental Sustainability Assessment of Solar Photovoltaic Technology in Nigeria: Rural Electrification Perspective," International Journal of Smart grid, vol. 7, no. 2, Jun. 2023, doi: 10.20508/ijsmartgrid. v7i2. 282.g280.

[25] X. Wang, L. Xia, C. Bales, X. Zhang, B. Copertaro, S. Pan, J. Wu, "A systematic review of recent air source heat pump (ASHP) systems assisted by solar thermal, photovoltaic, and photovoltaic/thermal sources", Renewable Energy, vol 146, pp. 2472-2487, 2020.

[26] P. Geetha, S. Ajitha, M. Jyothirmayi, T. Guha, A. Chaturvedi, P. Ganeshan, S. Taqui, E. A. Al-Ammar, S. Wabaidur, A. Iqbal, "Smart Operating Range Monitoring of Solar PV Cell with Integrated Phase Change Materials by Using Solar Deep Learning Model", Electric Power Components and Systems, vol. 52, no. 11, pp. 2147-2158, 2024, DOI: 10.1080/15325008.2023.2249882.

[27] J. Garcia, A. Rosa, "Theoretical Study of an Intermittent Water-Ammonia Absorption Solar System for Small Power Ice Production", Sustainability, vol. 11, no. 12, p. 3346, 2019, https://doi.org/10.3390/su11123346.

[28] N. Alvarenga, J. Martins, J. Caeiro, J. Garcia, J. Pássaro, L. Coelho, M. Santos, C. Lampreia, A. Martins, J. Dias, "Applying Computational Fluid Dynamics in the Development of Smart Ripening Rooms for Traditional Cheeses", Foods, vol. 10, no. 8, p. 1716, July 2021, https://doi.org/10.3390/foods10081716.

[29] V. Yakhot, S. Orszag, "Renormalization Group Analysis of Turbulence I Basic Theory", Journal of Scientific Computing, vol. 1, no. 1, pp. 3–51, 1986.

[30] V. Jayaram, B. Bavanish, M. Fahad, P. A. Azeem Hafiz, N. A. Salam, "Performance Evaluation of a Mini–Vertical Axis Cross Flow Helical Turbine meant for Energy Extraction from Dam's Tailrace," International Journal of Renewable Energy Research, vol. 14, no. 3, pp. 1-10, Sept. 2024, doi: 10.20508/ijrer.v14i3.14359.g8918.

[31] P. Agus Setiawan, T. Yuwono, W. Aries Widodo, E. Julianto, M. Santoso, K. Sukolilo Surabaya, "Numerical Study of a Circular Cylinder Effect on the Vertical Axis Savonius Water Turbine Performance at the Side of the Advancing Blade with Horizontal Distance Variations", International Journal of Renewable Energy Research, vol. 9, no. 2, pp. 1-8, June 2019, doi: https://doi.org/10.20508/ijrer.v12i4.13433.g8617.

[32] B. Launder, D. Spalding, "Lectures in Mathematical Models of Turbulence", Academic Press, London, England, 1972.

[33] T. Shih, W. Liou, A. Shabbir, Z. Yang, J. Zhu, "A New k-ε Eddy Viscosity Model for High Reynolds Number Turbulent Flows - Model Development and Validation", Computers & Fluids, vol. 24, no. 3, pp. 227–238, 1995.

[34] F. Saat, A. Jaworski, "Numerical Predictions of Early-Stage Turbulence in Oscillatory Flow across Parallel-Plate Heat Exchangers of a Thermoacoustic System", Applied Sciences, vol. 7, no. 7, p. 673, June 2017, https://doi.org/10.3390/app7070673.